Yuzuncu Yil University Journal of the Institute of Natural & Applied Sciences

https://dergipark.org.tr/en/pub/yyufbed

Research Article

Investigating the Origin of Microearthquakes around Tendürek Volcano (Eastern Türkiye) using Focal Mechanism Solutions and Stress Changes

Ayşegül ALKAN [1], İsmail AKKAYA[2], Hamdi ALKAN[*2]

[1] Graduate School of Natural and Applied Sciences, Van Yüzüncü Yıl University, Van, Türkiye
[2]Department of Geophysical Engineering, Faculty of Engineering, Van Yüzüncü Yıl University, Van, Türkiye

*Corresponding author e-mail: hamdialkan@yyu.edu.tr

Abstract: Tendürek Volcano is one of the Quaternary volcanic edifices in Eastern Anatolia. Its volcanic activity has been directly controlled by active regional tectonics since the Late Miocene. In and around Tendürek Volcano, several tectonic units are present, including the Tendürek Fault with a normal fault component and the Balıkgölü Fault Zone with a strike-slip fault component. Both the faults and the volcano are capable of generating local seismicity in the region. In this study, 22 low-magnitude seismic events ($M_L \leq 2.6$) that occurred around Tendürek Volcano were selected to identify and interpret the source of regional seismicity. Focal mechanism solutions for these events were determined using the FPFIT and PINV algorithms, and Coulomb stress changes were calculated from the focal mechanism solutions at different depths. The results, integrated with focal mechanism solutions and Coulomb stress modeling, indicate that positive stress values are concentrated beneath the volcano at shallow depths and extend westward and northeastward across the study area. Ultimately, these findings provide crucial insights into the structural characteristics of the volcanic environment and its interaction with local tectonics.

Keywords: Tendürek Volcano, Focal Mechanism, Stress Change, Seismicity

Tendürek Volkanı (Doğu Türkiye) Civarındaki Mikrodepremlerin Kökeninin Odak Mekanizması Çözümleri ve Gerilme Değişimi ile Araştırılması

Öz: Tendürek Volkanı, Doğu Anadolu'da yer alan Kuvaterner yaşlı volkanik kütlelerden biridir. Volkanik etkinliği, Geç Miyosen'den itibaren bölgesel tektonik süreçler tarafından doğrudan kontrol edilmiştir. Tendürek Volkanı ve çevresinde, normal bileşenli Tendürek Fayı ile doğrultu atımlı bileşene sahip Balıkgölü Fay Zonu gibi çeşitli tektonik yapılar bulunmaktadır. Bu faylar ve volkan, bölgedeki yerel depremselliğin oluşumundan sorumlu olabilecek yapısal birimlerdir. Bu çalışmada, Tendürek Volkanı civarında meydana gelen 22 adet düşük magnitüdlü ($M_L \leq 2.6$) deprem seçilerek bölgesel depremselliğin kaynağını belirlemek ve yorumlamak amaçlanmıştır. Seçilen depremlerin odak mekanizması çözümleri FPFIT ve PINV algoritmaları kullanılarak hesaplanmış, ayrıca farklı derinliklerde Coulomb gerilme değişimleri belirlenmiştir. Elde edilen sonuçlar, odak mekanizması çözümleri ve Coulomb gerilme modelleriyle birlikte değerlendirildiğinde, volkanın altındaki sığ seviyelerde pozitif gerilme değerlerinin yoğunlaştığı ve bu değerlerin çalışma alanının batı ve kuzeydoğu kesimlerine doğru yayıldığı görülmüştür. Sonuç olarak, bu bulgular volkanik ortamın yapısal özelliklerinin ve yerel tektoniklerle etkileşiminin anlaşılmasına önemli katkılar sağlamaktadır.

Anahtar Kelimeler: Tendürek Volkanı, Odak Mekanizması, Gerilme Değişimi, Depremsellik

Received Date: 29.09.2025
Accepted Date: 10.02.2026

How to cited: Alkan, A., Akkaya İ., Alkan H. (2026). Investigating the Origin of Microearthquakes around Tendürek Volcano (Eastern Türkiye) using Focal Mechanism Solutions and Stress Changes. *Yuzuncu Yil University Journal of the Institute of Natural and Applied Sciences, 31:108-125* https://doi.org/10.53433/yyufbed.1793064

1. Introduction

The Anatolian Plate (AP) is part of the Alpine-Himalayan Orogenic Belt. Since the Early Miocene, it has shifted westward (~24 mm/yr) and also undergone a counterclockwise rotation due to the northward movements of the Arabian (~13 mm/yr) and African Plates (~10 mm/yr), with the Eurasian Plate (~5 mm/yr) moving southward (Şengör & Yılmaz, 1981; Şengör et al., 2005; Reilinger et al., 2006; Zhou et al., 2025). The ongoing convergence throughout the Bitlis-Zagros Suture Zone (BZSZ) results in the uplift (about 2 km) of the Eastern Anatolian Plateau (EAP). The EAP is linked to this continental collision along the BZSZ, which began during the Eocene-Miocene periods, along with the major strike-slip faults such as the North Anatolian Fault (NAF) and East Anatolian Fault (EAF), and their interactions (Gülyüz et al., 2020). The NAF and EAF intersect at the Karlıova Triple Junction (KTJ) (Figure 1). Volcanic activity in the EAP began during this period (~11 Ma ago), characterized by collision-related volcanism between the BZSZ and Erzurum-Kars Plateau (Özdemir et al., 2006; Özdemir et al., 2019; Kearney et al., 2025). Young volcanism developed along extensional fractures, combined with a compressional/extensional regime that occurred approximately north-south, corresponding to the Neogene-Quaternary period, composed of alkali basalts and normal alkalinity basalts to rhyolites and trachyrhyolites (Lebedev et al., 2016a). In this region, the volcanic belt is represented by shield volcanoes (Tendürek) and stratovolcanoes (Ağrı, Süphan, Nemrut), which developed in an extensional tectonic regime during the Quaternary period (Koçyiğit et al., 2001; Keskin, 2003; Şengör et al., 2008).

The characteristic features of volcanoes in different regions of the world are investigated in detail using various seismic and seismotectonic parameters, such as Coulomb stress changes, *b*-value variations, and focal mechanism solutions. In recent years, numerous studies have been conducted to explore the relationship between volcanic activity and seismic activity (Tilling & Dvorak, 1993; Toda et al., 2002; Troise et al., 2003; Foulger et al., 2004; Gargani et al., 2006; Massa et al., 2016; Alkan et al., 2023; Büyüksaraç et al., 2024; Chen et al., 2024).

The Tendürek Volcano is located south of the Ağrı Volcano and near the Iran-Türkiye border, with Çaldıran to the south and Diyadin to the northwest. It is an isolated, polygenetic, two-peaked volcano consisting of Greater Tendürek and Lesser Tendürek, separated by a half-caldera and a classic basaltic shield volcano. This volcano features alkaline volcanism mainly composed of basaltic-trachytic rocks (Lebedev et al., 2016a; Ulusoy, 2016; Ünal, 2018). The Greater Tendürek reaches about 3,540 meters in altitude, while the Lesser Tendürek stands around 3,300 meters with well-preserved craters (Yılmaz et al., 1998; Lebedev et al., 2016a; Lebedev et al., 2016b; Alkan, 2022). Lava flows from Tendürek extend approximately 10 km from Doğubeyazıt in the north to Çaldıran in the south. Surrounding the volcanic center, there are Paleozoic metamorphic rocks in the south, ophiolitic mélanges in the north, and Pliocene carbonate and clastic formations in the northwest (Lebedev et al., 2016a; Lebedev et al., 2016b). Pliocene volcanism, linked to collision processes, is dominant in this area. Evidence of Quaternary volcanism around Tendürek includes eruptive products like basalts and trachybasalts (Pearce et al., 1990; Lebedev et al., 2016a; Lebedev et al., 2016b).

The main tectonic structures around the Tendürek Volcano are the Erciş, Çaldıran, Süphan, Nemrut, Nazik Gölü, Malazgirt, Yeniköşk, and Saray faults and fault zones (Figure 2a). A right-lateral strike-slip mechanism controls the Erciş, Çaldıran, Nazik Gölü, and Saray fault zones. Whereas the Süphan and Malazgirt faults are primarily characterized by a left-lateral strike-slip mechanism. However, the Yeniköşk Fault and the Van Fault Zone are generally controlled by reverse fault mechanisms trending in an E-W direction. In contrast, the extensional fractures of the Nemrut and Tendürek faults are characterized as normal fault systems (Emre et al., 2018).

Volcanic activity has not been observed since 1855 at the Tendürek Volcano (Karakhanian et al., 2002; Gündüz et al., 2023). In addition, an eruption occurred in the region around 550 BC. Despite the lack of ground observations, recent radar imagery has shown that Tendürek Volcano is subsiding at a rate of about 1 cm per year (Bathke et al., 2013; Bathke et al., 2015). During the instrumental period, earthquake locations have been concentrated in the southern and southeastern parts of the volcano. Especially, the 1976 Çaldıran earthquake (M_S=7.3) and the 2011 Van earthquake (M_W=7.2) were great earthquakes in the region (Alkan & Bayrak, 2022; Öztürk & Alkan, 2023). These earthquakes caused massive loss of life and left large numbers of people homeless. Conversely, the faults and fault zones near the volcano generally produced small-magnitude earthquakes. In Figure 2b, the epicenter

distribution of approximately 19,000 earthquakes is shown in the study region between 1900 and 2025. Many of these earthquakes were aftershocks of the 2011 Van earthquake (M_W=7.1). In addition to this information, small-magnitude earthquakes also occurred along the main faults and fault zones.

In this study, the first aim is to present the focal mechanisms of microearthquakes that occurred around the Tendürek Volcano, northeast of Lake Van. Because stress change plays an important role in earthquake triggering and clustering, the second aim is to investigate the Coulomb stress changes at the different depth intervals using focal kinematic parameters (e.g., strike, dip, slip angle, depth, and magnitude), which are very useful for inferring stress transfer. The third aim is to identify tectonic structures with earthquake potential in the future by utilizing the stress field around the Tendürek Volcano. The final objective is to determine whether these stress changes are related to volcanic activity or local tectonic structures. Therefore, the identification of the seismic activity around the Tendürek Volcano will contribute to defining the seismicity of other volcanoes.

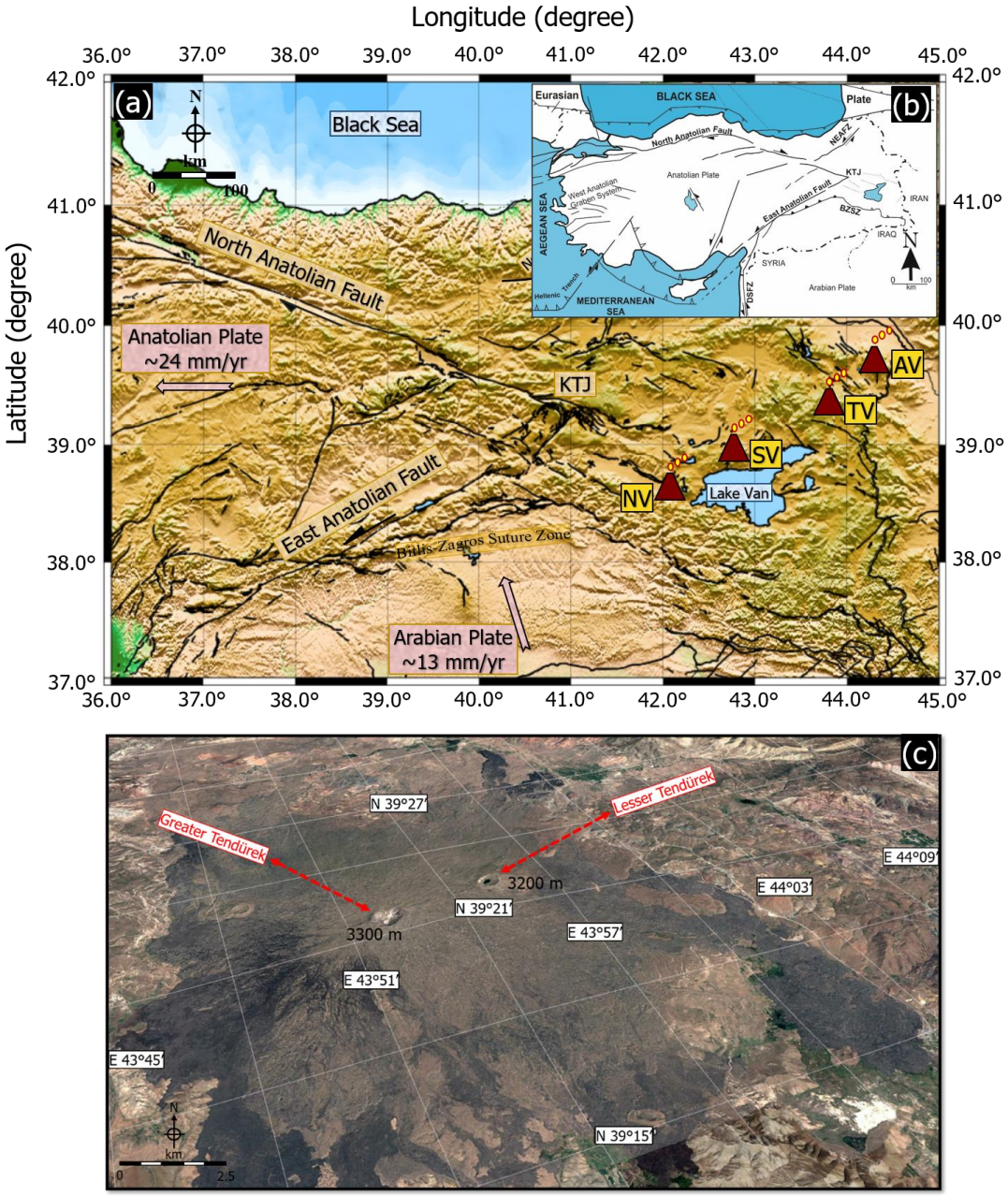

Figure 1. (a) Active tectonic elements of Eastern Anatolian Plateaus (modified after Şengör et al. (2003), Emre et al. (2018), Alkan et al. (2024), Büyüksaraç et al. (2024) and Bektaş et al. (2025)). Clared red triangles indicate Quaternary volcanic centers. Pink arrows show plate movement directions in mm/yr

(modified after Reilinger et al., 2006). The topography model was taken from the National Oceanic and Atmospheric Administration (NOAA). The figure is created using GMT (Wessel et al., 2019). (b) The map shows the major tectonic zones of Anatolia. Active fault zones in the region are modified from Emre et al. (2018). (Abbreviations: AV: Ağrı Volcano, KTJ: Karlıova Triple Junction, NV: Nemrut Volcano, SV: Süphan Volcano, TV: Tendürek Volcano). (c) A 3D perspective view of the Greater and Lesser Tendürek is provided by Google Earth Pro.

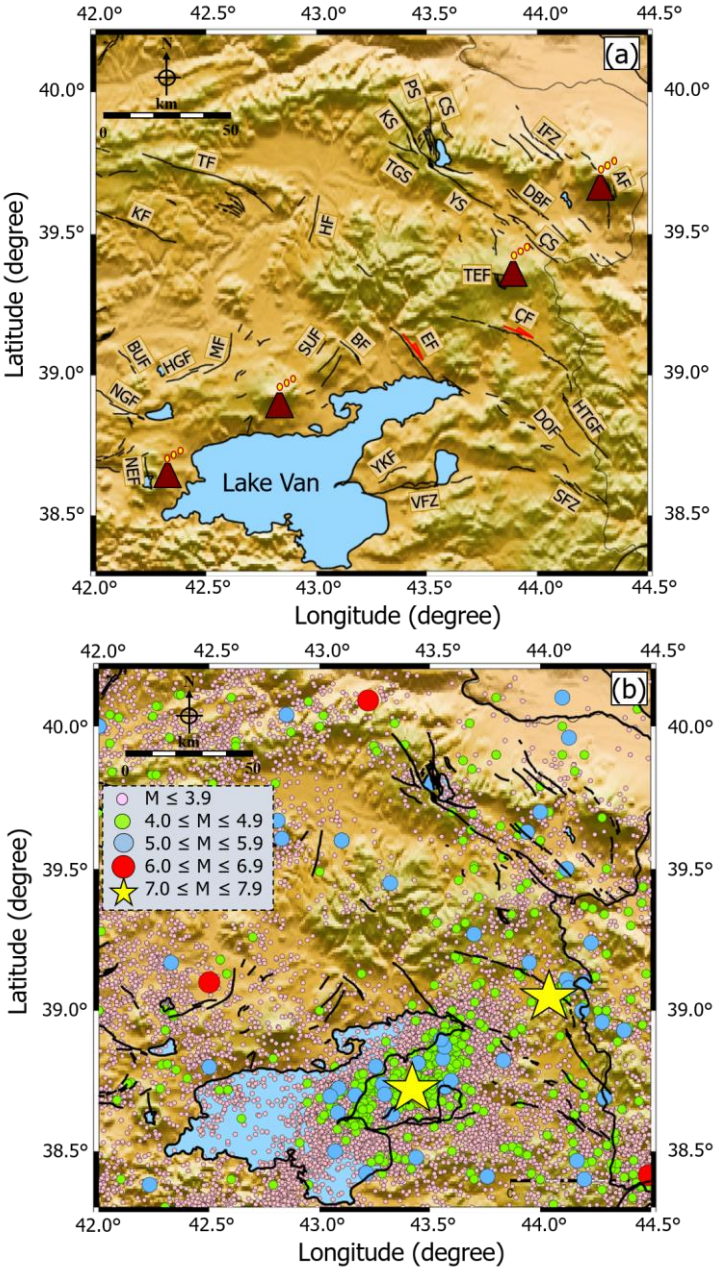

Figure 2. (a) Active faults in the study region, modified from Emre et al. (2018). Abbreviations: AF: Ağrı Fault, BF: Bulamaç Fault, BUF: Bulanık Fault, CS: Candervis Segment, ÇF: Çaldıran Fault, ÇS: Çetenli Segment, DBF: Doğubeyazıt Fault, DOF: Dorutay Fault, EF: Erciş Fault, HF: Hamur Fault, HGF: Haçlı Gölü Fault, HTGF: Hasantimur Gölü Fault, IFZ: Iğdır Fault Zone, KF: Kazbel Fault, KS: Kovancık Segment, MF: Malazgirt Fault, NEF: Nemrut Fault, NGF: Nazik Gölü Fault, PS: Perilidağ Segment, SFZ: Saray Fault Zone, SUF: Süphan Fault, TF: Tutak Fault, TEF: Tendürek Fault, TGS: Tirso Gölü Segment; VFZ: Van Fault Zone, YKF: Yeniköşk Fault, YS: Yeniçadır Segment. (b) Epicenter locations of 19,000 earthquakes with M≥1.0 from 1900 to 2025 for the study region. The

seismicity catalog was obtained from the KOERI website (https://udim.koeri.boun.edu.tr/). The magnitudes of the events are plotted using different symbols. The figures are created using GMT (Wessel et al., 2019). The topography model was taken from the National Oceanic and Atmospheric Administration (NOAA).

2. Data and Methods

2.1. Data

Focal mechanism solutions for earthquakes with magnitudes smaller than M_L<4.0 are usually unavailable in Türkiye, mainly due to data limitations and the heavy workload of earthquake research institutes. Additionally, focal mechanism solutions of microearthquakes occurring around Tendürek Volcano are typically absent. When examining earthquakes that occurred particularly around the Tendürek Volcano after 2000, two moderate earthquakes (2015, M_W=4.0) occurred near the Doğubeyazıt Fault (AFAD, 2025). On the other hand, the digital data capacity increased in parallel with the increase in the number of earthquake stations over the years. Therefore, due to the absence of large magnitude earthquakes and the current time interval, events were checked around the Tendürek Volcano between 2020 and 2025.

The careful selection of earthquakes is crucial, considering the earthquake-generating potential of active faults and fault zones within and around Tendürek Volcano. To address this issue, we collected three-component records from broadband stations operated in the region by the Disaster and Emergency Management Authority (AFAD). The nine broadband stations in the study area are shown in Figure 3, with detailed information provided in Table 1. Between July 2020 and December 2025, a total of 59 microearthquakes occurred near Tendürek Volcano. Their local magnitudes ranged from 0.8 to 2.6, with an epicentral depth of approximately 7.0 km (AFAD, 2025). 3-component seismograms from these stations were analyzed to derive focal mechanism solutions. Considering station establishment dates, active periods, truncated records, and low S/N ratios, a total of 22 microearthquakes could be selected for the data processing. If the selected earthquakes were recorded at least six stations, the RMS errors and azimuthal gaps would be minimal, leading to more accurate solutions.

Before calculating the focal mechanisms, a series of preliminary data processing steps was applied to the miniseed formatted 3-component records. These steps included removing instrument response, detrending, tapering, and Butterworth bandpass filtering. For the data preprocessing, the seismic analysis code (SAC) was used (Helffrich et al., 2013). After these preprocessing steps, the first arrivals of the P-phase and S-phase with their polarities and highest amplitudes became visible in the three-component seismograms. Figure 4 shows the vertical (Z) and horizontal (N and E) components at the DYDN station for event no. 14 in Table 2. This event has a normal component fault mechanism with an epicenter depth of 10.8 km and a local magnitude of 2.5. These steps for all earthquakes given in Table 2 can be found in Alkan (2026).

Table 1. Catalog information of broadband earthquake stations used in the study region and operated by the AFAD website (https://deprem.afad.gov.tr/stations).

Station Code	Latitude (N°)	Longitude (E°)	Elevation (m)	Sensor Type	Opening Time (dd/mm/yyyy)
DYDN	43.688	39.543	2010	CMG-3T	15/07/2006
IGDI	44.078	39.868	860	CMG-3T	23/01/2012
VMUR	43.571	38.989	1717	CMG-3T	29/11/2010
KOTA	43.205	39.802	1822	CMG-3T	05/12/2014
DORK	42.780	39.387	1714	CMG-3ESPC	09/11/2017
ADCV	42.724	38.808	1774	CMG-3T	28/10/2011
EATA	42.491	39.862	2770	CMG-3T	06/10/2009
OZAP	43.992	38.661	2058	CMG-3T	27/11/2014
DOGU	44.043	39.655	1571	CMG-3ESPC	19/01/2024

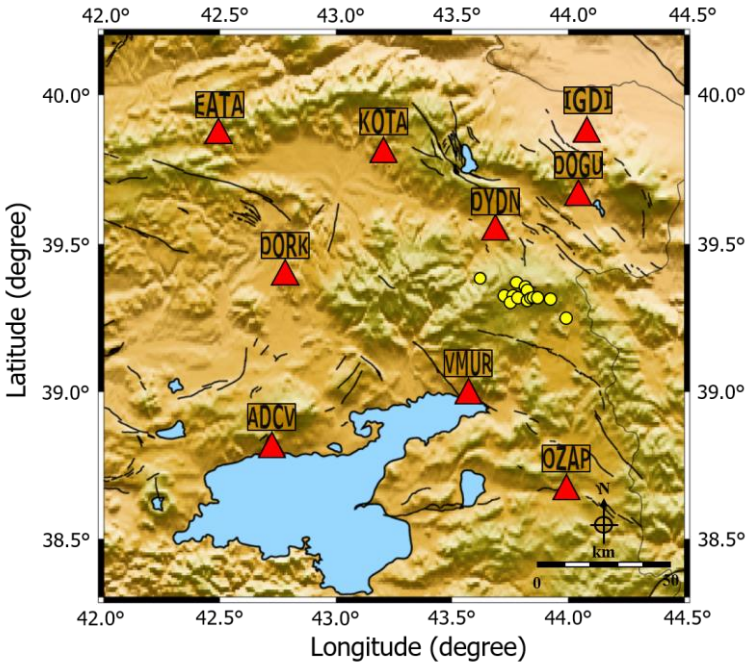

Figure 3. The selected broadband stations (shown as red triangles) are operated by the AFAD. The yellow circles represent epicentral locations of selected microearthquakes that occurred between 2020 and 2025 around the Tendürek Volcano. Earthquake and station locations were taken from AFAD's database (https://www.afad.gov.tr/). Active faults were modified from Emre et al. (2018). The topography model was taken from the National Oceanic and Atmospheric Administration (NOAA). The figure is created using GMT (Wessel et al., 2019).

2.2. Calculation of focal mechanism solution

SEISAN is an earthquake analysis software that can perform phase readings (arrival times, amplitude, period, azimuth, and apparent velocity) of both local and global earthquakes. The system includes several programs to calculate spectral parameters, seismic moments, azimuths, and epicenter locations using three-component seismograms. SEISAN enables manual phase readings of selected seismograms or the automatic detection of seismic phases (Ottemöller et al., 2021). The SEISAN software package is a comprehensive set of tools for analyzing both analog and digital earthquake data.

To calculate the fault plane solution, which comprises fault orientation and slip direction, the FPFIT (Reasenberg & Oppenheimer, 1985) and PINV (Suetsugu, 1998) software packages were used. FPFIT and PINV are part of SEISAN (Ottemöller et al., 2021). The FPFIT determines the double-couple fault plane solution (source model) by observing P-wave first-motion polarities for an earthquake. The inversion is based on a two-stage grid search procedure and a weighted sum of first-motion polarities to identify the best-fitting focal mechanism (Kilb & Hardebeck, 2006). This technique minimizes the residuals between the nodal planes and the observed first-motion data (Tahir et al., 2024). Confidence intervals are determined by finding each parameter (strike, dip, and rake) that does not exceed a critical misfit level (Hardebeck & Shearer, 2002). On the other hand, PINV, developed by Suetsugu (1998) provides a preliminary fault plane solution based on P-wave polarities. This algorithm is to help solve FPFIT. It is not recommended to primarily use the solutions of PINV as a fault plane solution. RMS values are important parameters of the focal mechanism solutions, shown in Table 2. Snoke (2003) stated that for each solution that meets the specified criteria, the solution gives the number of ratios for which there is no ratio error greater than the cut-off. Therefore, the RMS errors of the acceptable ratios are acceptable for each solution. In this study, we considered the visible phases of P- and S-wave arrivals with maximum amplitudes in horizontal amplitudes and adjusted the RMS values to be less than 5.00.

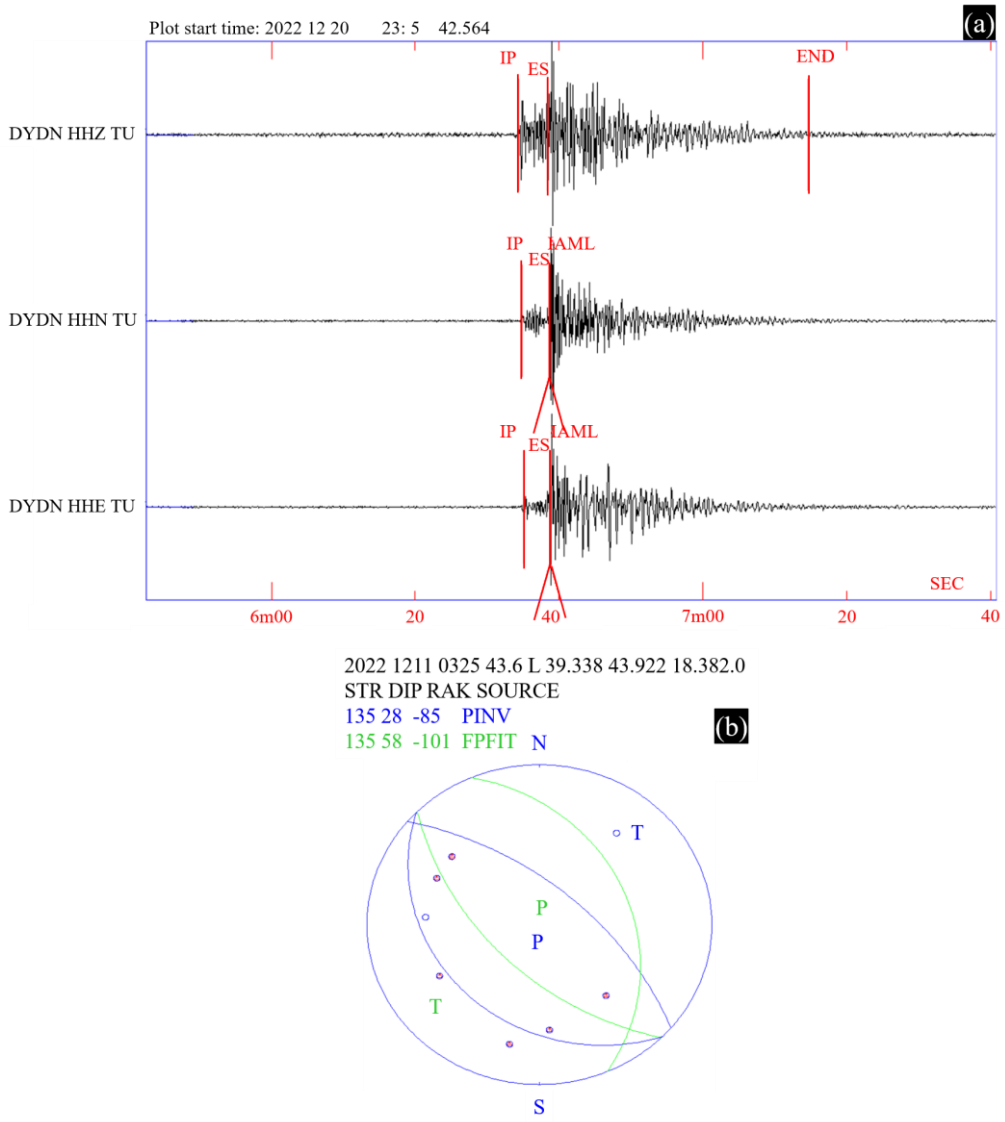

Figure 4. (a) The 3-component seismograms at the DYDN station for event no. 14 in Table 2. After the preliminary data processing steps, the P-phase (IP), S-phase (ES), maximum amplitude (IAML), and duration (END) can be clearly observed. (b) Focal mechanism solution of event no. 14 in Table 2. The blue solution is related to PINV and the green solution to FPFIT. Tensional and compressional axes are also shown as T and P, respectively.

2.3. Coulomb stress change

Since any earthquake can influence subsequent earthquakes, it is important to understand interactions among faults and active volcanoes. These interactions are calculated using Coulomb Failure Stress (ΔCFS), which measures the Coulomb stress change based on source and receiver fault parameters, geometries, and slip directions (Wang et al., 2014). By analyzing ΔCFS, it is possible to identify different sources at various depths and geometries under the failure conditions (King et al., 1994). Modeling the stress change related to tectonic and volcanic regions is commonly used and provides information about local seismic activity. According to the Coulomb rupture criterion, failure occurs when the stress change exceeds the strength of rocks along the fault (Asayesh et al., 2020). ΔCFS can be defined as:

$$\Delta CFS = \Delta\tau + \mu(\Delta\sigma_n + \Delta P) \quad (1)$$

In this formula, $\Delta\tau$ is the shear stress change (positive when the slip direction is along the fault), $\Delta\sigma_n$ is the normal stress change (positive for extension), ΔP is the pore pressure change (positive for compression), and μ (dimensionless) is the effective coefficient of friction, which ranges from 0 to 1. μ is approximately 0.4 under moderate pore pressures (King et al., 1994; Yue et al., 2025). The frictional coefficient is a key parameter that influences the determination of ΔCFS. Although the degree of heterogeneity varies among different type volcanic systems, the coefficient of friction was used as 0.4 in previous studies (Feuillet et al., 2006; Cailleau et al., 2007; Miller et al., 2017; Lin et al., 2025). Based on this assumption, a similar friction value was used in this study. The medium is assumed as a homogeneous elastic half-space, with values of $8x10^5$ (bars) for Young's modulus, $3.3x10^5$ (bars) for Shear modulus, and 0.25 for Poisson's ratio (dimensionless). Positive ΔCFS promotes failure, and negative inhibits it. In this study, the Coulomb stress changes were calculated using the Coulomb 3.3 software (Toda et al., 2011). A workflow diagram is shown in Figure 5, composed of the preliminary raw data processing, the determination of the focal mechanism solutions, and the creation of the Coulomb stress change maps with cross-sections.

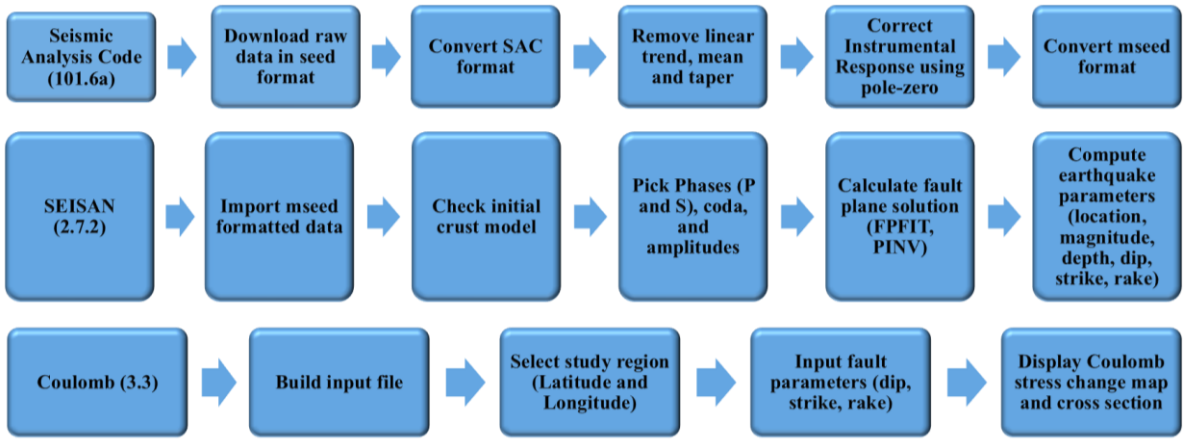

Figure 5. Workflow diagram about the preliminary raw data processing using Seismic Analysis Code 101.6a (Helffrich et al., 2013), SEISAN 2.7.2 (Ottemöller et al., 2021), and Coulomb 3.3 (Toda et al., 2011).

3. Results and Discussion

In volcanic regions, it is crucial to distinguish between seismic activity resulting from tectonic processes and volcanic activity. A time-seismic analysis of activity before and after volcanic eruptions is necessary to understand the interaction between tectonic and magmatic processes (Gargani et al., 2006). To examine the relationship between local events linked to volcanism and tectonism, it is essential to calculate the focal mechanism parameters and Coulomb stress variations as a function of depth. Stress changes play a key role in fluid migration along the shallow crust and may be responsible for tectonic earthquakes (Massa et al., 2016). In this study, Coulomb stress changes were calculated using 22 earthquakes with magnitudes ranging from $1.2 \leq M_L \leq 2.6$ and focal depths from $3.9 \leq H \leq 22.9$, occurring around Tendürek Volcano. The spatial and depth distribution of the selected earthquakes revealed that the events were not interconnected with a specific main shock-aftershock sequence, but rather occurred within the 2020–2025 time period. Spatially, these events occurred around the Tendürek Volcano, particularly near the Tendürek Fault, the Balıkgölü Fault Zone, and the Doğubeyazıt Fault. These locations indicated that the selected events were associated with active tectonic and volcanic structures in the region. The AFAD instrumental period earthquake catalog (AFAD, 2025) showed that the number of earthquakes greater than $M_L \geq 4.0$ around the Tendürek Volcano is quite low. In addition, earthquakes with $M_L \leq 3.9$ had similar characteristics to events of this study and occurred in a scattered manner rather than in clusters. On the other hand, the focal parameter solutions of these local events are shown in Table 2 and Figure 5. The focal mechanism solutions obtained in this study clearly show that, rather than a single uniform deformation regime, normal, strike-slip, and thrust/oblique-thrust faulting coexist in and around Tendürek Volcano (Figure 6). In particular, normal and thrust fault mechanisms

are concentrated at shallow levels of the volcano and in areas associated with the caldera and ring-fault systems. This kinematic diversity indicates that the focal mechanism data reflect a heterogeneous deformation field beneath Tendürek Volcano and that both tectonic and volcanic processes influence the seismic activity.

Coulomb stress change maps at different depths (4, 8, 12, and 16 km) are shown in Figure 7, and the cross-section profiles (A-B and C-D) are displayed in Figure 7. Earthquake epicenters (green circles) are marked on the maps to examine the relationship between Coulomb stress variations and the locations of epicenters. Positive and negative stress changes provide insight into potential volcano-tremors and future seismic hazards in the region. The Coulomb stress map at a depth of 4 km (Figure 7a) reveals that positive and negative stress lobes extend in the E-W direction. The negative stress values were observed around the Tendürek Volcano, whereas positive stress changes were detected at earthquake epicenters located to the west, which are reported for the first time in this study. Additionally, positive stress values occurred near the Tendürek Fault, the Balıkgölü Fault Zone, and the Doğubeyazıt Fault in the northeastern part of the study area. Conversely, moderate to low stress levels were recorded around the Çaldıran and Erciş faults.

In Figures 7b and 7c, the stress changes at depths of 8 and 12 km show positive lobes in the northern part of Tendürek Volcano, which may be associated with the Tendürek Fault and local volcanism. Additionally, moderate to high-stress values were observed in the northeastern part of the region, near the Balıkgölü and Doğubeyazıt faults. These faults have not generated any recent destructive or damaging earthquakes in the instrumental period, except for moderate magnitudes (AFAD, 2025). Öztürk (2017, 2018) analyzed the regional characteristics of seismicity in the Eastern Anatolian region using various statistical parameters, including *b*-value, *Z*-value, *Dc*-value, and seismic quiescence. The moderate *b*-value (~1.0) and *Dc*-value (~2.2) were calculated around the Tendürek Volcano, comprising the Doğubeyazıt Fault Zone, Balıkgölü Fault Zone, Ağrı Fault, and Iğdır Fault. When examining the epicenter and hypocenter locations of the selected microearthquakes, no microearthquakes were detected around the Çaldıran and Erciş faults. Therefore, no anomalies were identified in this region. This situation results from the data analyzed in this study. In fact, it is known that many earthquakes have occurred in this region during the instrumental and historical periods.

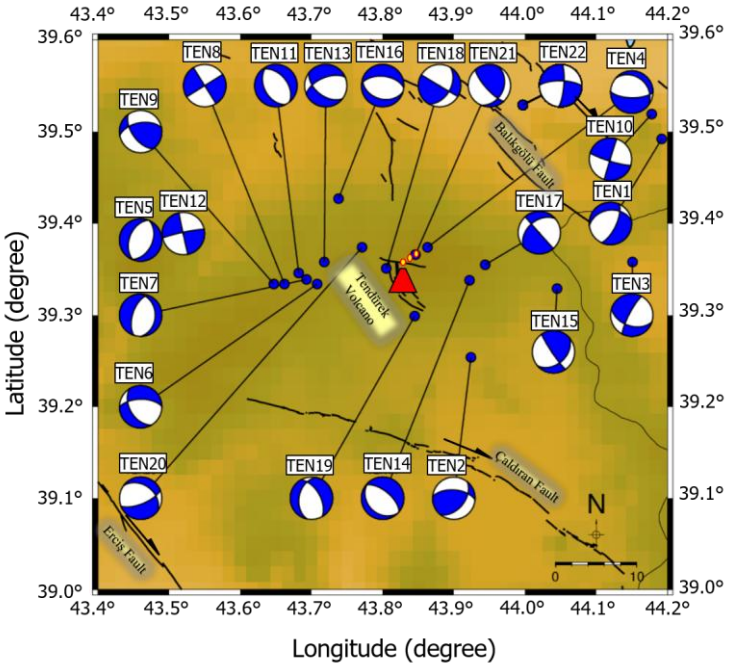

Figure 6. Focal mechanism solutions for 22 microearthquakes that occurred near Tendürek Volcano (shown as blue beach balls). For detailed information, please see Table 2. Active faults were modified from Emre et al. (2018).

Table 2. Focal mechanism solutions of microearthquakes occurring between 2020 and 2025 around the Tendürek Volcano (Lat: Latitude, Long: Longitude, AZ: Azimuth, OBS: Observation, S/D/R: Strike/Dip/Rake).

No	Date (dd/mm/yy) (hh:mm:ss)	Lat (N°)	Long (E°)	Depth (km)	Mag (M_L)	RMS	Total OBS	Gap in AZ	S/D/R (°)	Fault Type
1	04/04/2025 18:00:56	39.492	44.192	7.0	2.0	2.00	14	146	25 68 -121	
2	15/03/2025 11:14:43	39.254	43.924	9.1	2.4	1.60	15	168	39 48 46	
3	21/12/2024 14:52:47	39.358	44.151	9.2	1.9	3.00	15	124	108 48 -147	
4	24/08/2024 00:18:44	39.374	43.863	7.8	1.5	3.00	12	113	91 68 -107	
5	14/09/2023 20:32:25	39.382	43.460	4.80	2.1	2.50	18	163	24 44 -88	
6	27/12/2022 11:51:18	39.334	43.708	8.1	1.3	1.40	16	123	149 48 -41	
7	22/12/2022 14:04:37	39.339	43.693	13.7	1.4	1.10	17	131	0 32 -106	
8	22/12/2022 12:15:11	39.334	43.662	4.1	2.5	1.30	19	129	-54 90 -89	
9	22/12/2022 11:19:33	39.334	43.647	3.9	1.9	1.40	13	123	144 58 138	
10	22/12/2022 02:03:01	39.519	44.178	7.06	2.2	4.70	13	110	107 82 -1	
11	21/12/2022 23:33:51	39.346	43.682	8.2	1.6	1.30	22	89	153 44 -81	
12	21/12/2022 20:34:40	39.389	43.497	6.5	1.2	2.40	14	131	258 85 1	
13	20/12/2022 23:06:29	39.358	43.718	15	1.4	2.10	12	121	128 51 -41	
14	11/12/2022 03:25:44	39.338	43.922	10.8	2.5	1.20	21	57	135 28 -85	
15	01/10/2022 05:16:10	39.329	44.045	22.9	2.3	2.00	12	129	49 41 171	
16	03/07/2022 01:10:36	39.427	43.738	18.8	1.6	1.60	13	85	107 37 -81	
17	10/05/2022 23:07:08	39.355	43.944	12	1.4	2.00	14	114	229 44 -179	
18	10/02/2022 03:02:08	39.351	43.805	19.8	2.0	1.80	16	94	30 47 -1	
19	12/12/2021 02:15:56	39.299	43.845	11.1	2.5	1.80	23	103	330 57 -116	
20	09/09/2021 23:43:42	39.374	43.771	10.3	2.3	1.40	15	110	68 68 -121	
21	04/09/2021 05:45:18	39.366	43.846	6.92	2.6	1.70	13	127	138 75 60	
22	01/07/2020 07:05:10	39.529	43.997	16.1	2.0	3.30	13	106	5 78 -161	

Overall, all figures indicate large negative lobes in the southern and southeastern regions of the volcano, with positive lobes in the western part of the area. Some of the earthquakes for which focal mechanism solutions were calculated in this study clearly occurred within positive-stress regions with earthquake clustering. These positive stress variations were likely associated with the selected microearthquakes. The focal depths of the earthquakes support this interpretation (see Table 2 and Figure 6). As depicted in Figure 7d for a depth of 16 km, the stress values caused by selected

microearthquakes decrease with increasing depth. On the western slopes of Tendürek Volcano, there is a known arc-shaped fracture system interpreted as the surface evidence of a ring fault that may have formed during a historical collapse event (Yılmaz et. al., 1998; Bathke et. al., 2015). The presence of active caldera ring faults at Tendürek Volcano may have produced local seismicity and stress fields in the region due to substantial westward-directed lateral movement (Troise et al., 2003; Bathke et al., 2015). The InSAR data reveal that the area within the ring-fault not only subsides, but also shows substantial westward-directed lateral movement (Bathke et. al., 2015). The ring faults of the caldera may be a normal or reverse fault and are related to the generation of the local stress field and loading conditions around the caldera (Gudmundsson et al., 1997). Additionally, Feuillet et al. (2006) noted that earthquakes in the Etna Mountain region created a vertical stress gradient along the large normal fault systems. The stress change becomes negative at increasing depths (≥16 km), and therefore, seismicity is low. Additionally, previous studies have determined that deformation at Tendürek Volcano occurs predominantly in the vertical direction, with a negligible horizontal deformation component (Gündüz, 2024). These InSAR-based studies reported a collapse of the summit caldera of approximately 11 mm/year (Bathke et al., 2013; Gündüz et al., 2023).

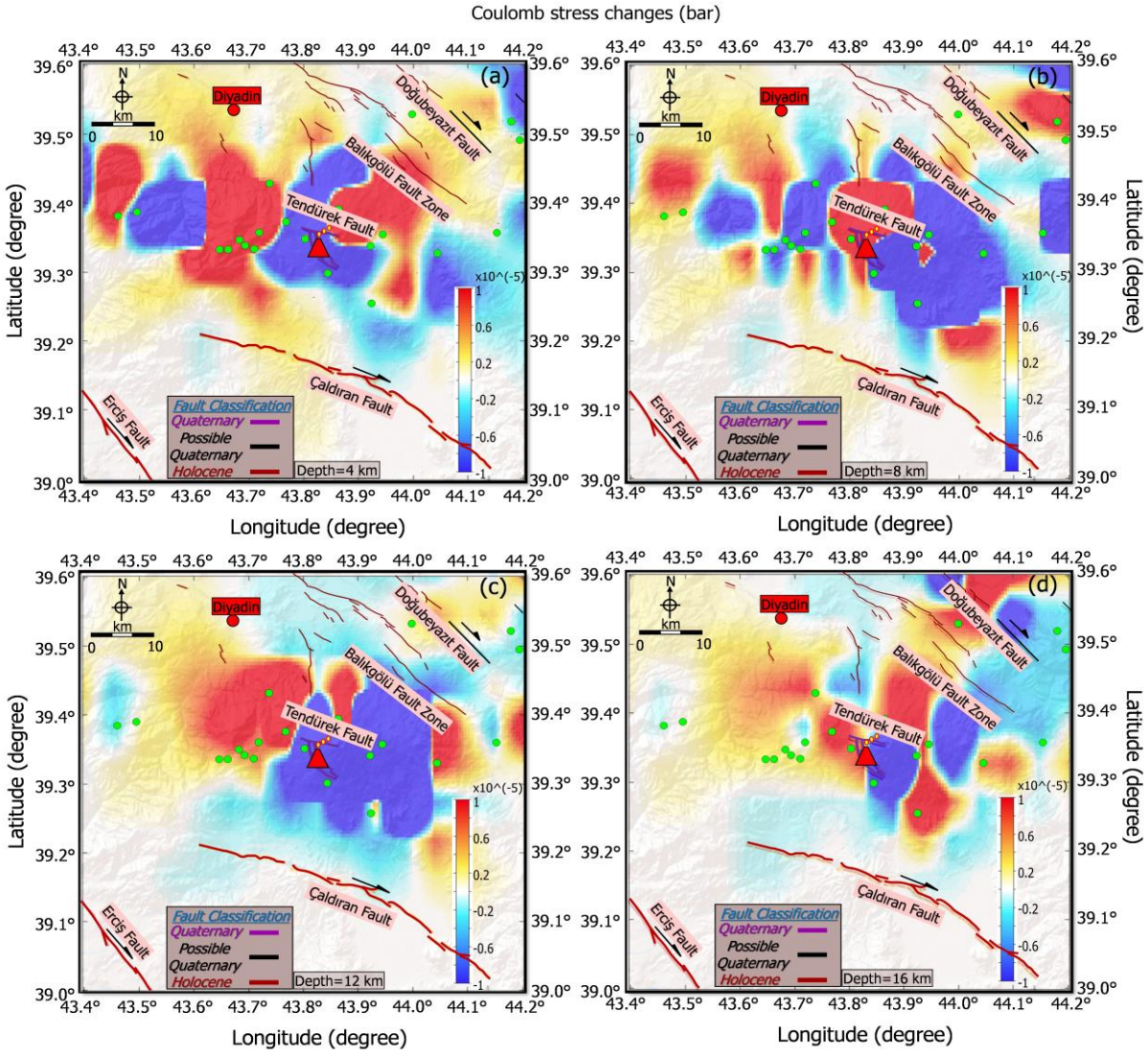

Figure 7. Coulomb stress change maps (in bars) based on focal mechanism solutions presented in Table 2. Depth levels are changed as (a) 4, (b) 8, (c) 12, and (d) 16 km. Active faults were modified from Emre et al. (2018). Green circles depict relocations of selected earthquakes. All calculations assumed an effective coefficient of friction (μ) of 0.4. The positive stress lobes are depicted in red colors, and the negative stress lobes are shown in blue colors. Active faults were modified from Emre et al. (2018).

In addition, it is emphasized that the subsidence observed in Tendürek Volcano can be explained by non-magmatic mechanisms such as crustal relaxation following volcanic processes and caldera-related structural movements. Therefore, the deformation is interpreted not as evidence of active magmatism, but as an indicator of the long-term geodynamic process ongoing beneath the caldera. These data are highly consistent with the positive stress changes obtained at shallow depths beneath Tendürek Volcano (Figure 8).

Figure 8 shows the cross-sections of stress changes along the NW-SE-trending A-B profile and NE-SW-trending C-D profile down to a depth of 20 km. Positive stress changes were observed beneath Tendürek Volcano at shallow depths (2-3 km), directed both upward and downward, although they appear scattered. These stress transfers may be linked to local volcanism with low-viscosity magma.

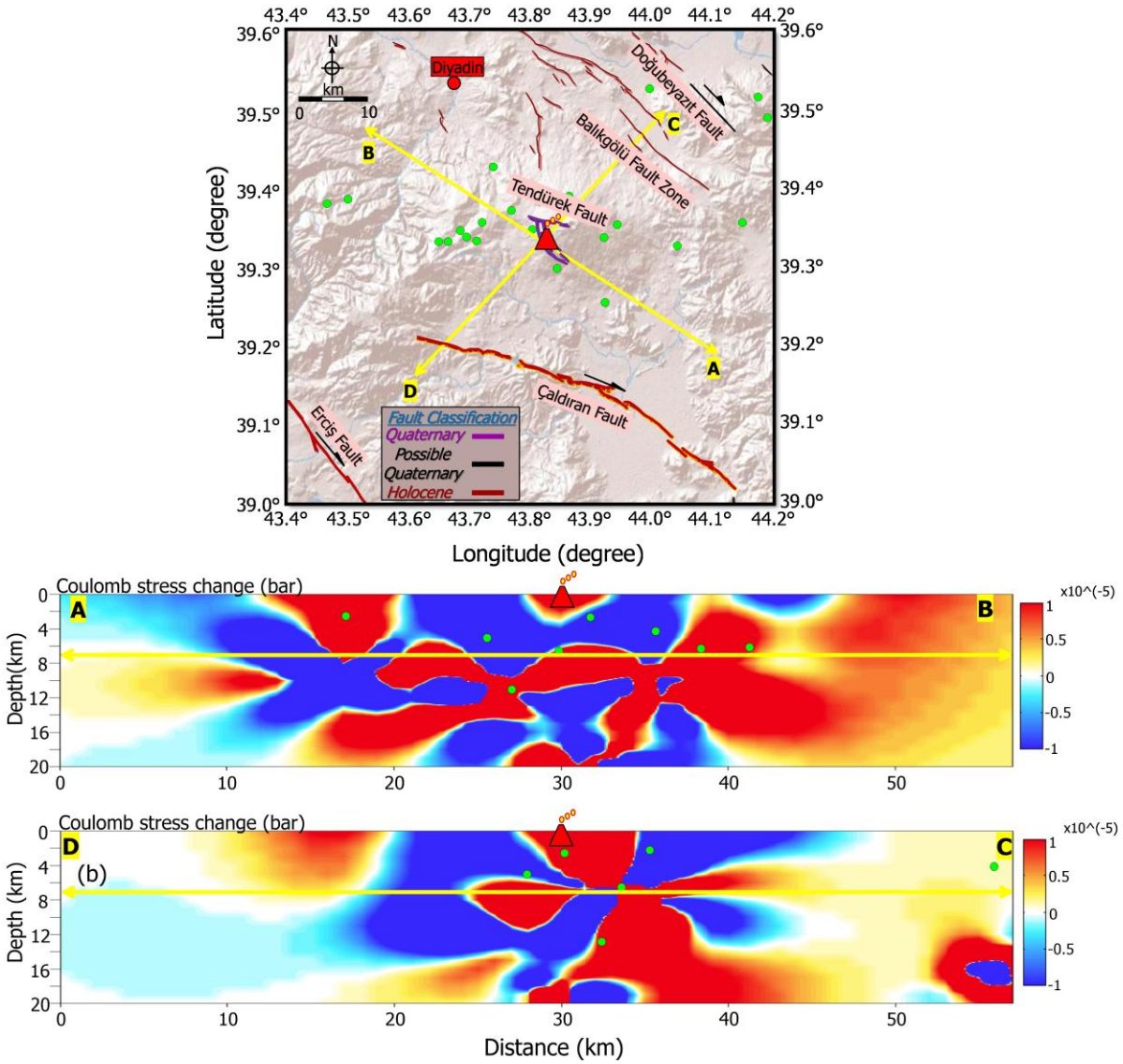

Figure 8. Cross-section profiles (A-B and C-D) of Coulomb stress change from 0 to 20 km around the Tendürek Volcano. Other details are the same as in Figure 7.

During the formation process of the Tendürek Volcano, the dominant rock type was low-viscosity, fluid basaltic lava erupting from the central vent (Pearce et al., 1990; Ercan et al., 1990; Şen et al., 2004), and the fact that it flowed easily, covering an area of 600 km^2 and having a product volume of 300 km^3 (Yılmaz et al., 1998) can explain the high stresses around the volcano. Dhar et al. (2025) stated that the existence of a small-scale low-viscosity zone beneath the Quaternary volcanoes in

northeastern Japan (Mt. Akitakoma, Mt. Kurikoma, Mt. Zao, Mt. Azuma, and Mt. Nasu) was linked to local ground motion activities in the region. It was suggested that these low-viscosity zones cause local crustal deformations around the Quaternary volcanoes. Also, Chen et al. (2024) reported that aftershocks in the south of the Coso Volcanic Field were distributed much deeper than those in the north of the volcano, which may affect the spatial pattern of seismic activity in this region due to low viscosity zones associated with magma reservoirs. The low-level thermal activity on the volcano (Ulusoy, 2016) is associated with these stress changes. Additionally, focal mechanism solutions exhibit predominantly normal fault characteristics. When reservoir pressure increases, positive stress values are observed beneath the volcanic chamber, which may have caused cracks and seismicity (Gargani et al., 2006). According to Alkan et al. (2024), normal fault mechanisms confirm the upward-downward stress variations. Moreover, the positive lobes are more prominent at 8 km depth along the northwest and northeast parts of the study area. Bektaş et al. (2007) and Akın et al. (2014) calculated a Curie point depth of ~18 km around the Ağrı and its surroundings. This region is associated with the widespread thermal activity and high heat flow value (~70 mW/m^2) over young volcanic rocks. Kiyak et al. (2023) showed that magmatic rocks have a high amplitude (0.01 and 0.047 nT/m) on the total horizontal derivative map. This stress variation results from the hypocenter depths and the types of focal mechanisms (normal and strike-slip) of the earthquakes listed in Table 2. In the western part of the region, no active fault is observed. It may be possible to infer some stress transfer, although with very low energy. Finally, the limited earthquake dataset in the region complicates the interpretation of local tectonic and volcanic activity; however, small stress changes can still provide insights into tectonic and volcanic processes.

4. Conclusion

In this study, we analyzed the microearthquakes occurring beneath and around Tendürek Volcano, located northeast of Lake Van. For this purpose, twenty-two earthquakes with high S/N ratios were selected. Focal mechanism solutions for these earthquakes were calculated using the SEISAN software (Ottemöller et al., 2021), and the stress changes were determined using Coulomb 3.3 software (Toda et al., 2011). The overall seismicity of the region indicates small-magnitude events, all with magnitudes less than 3.0. Therefore, Coulomb stress maps were generated for relatively small values (in bars). The presence of different faulting mechanisms in the obtained earthquake solutions reflects the complex stress regime of the region (see Figure 6). This situation is thought to result from the interaction between the regionally dominant N–S compressional regime in Eastern Anatolia, pressure changes associated with the magma reservoir, and the geometry of caldera/ring fault systems, leading to local-scale heterogeneity in the stress field around the Tendürek Volcano.

The 2D cross-sections and the Coulomb stress maps revealed scattered positive and negative stress values in the study region. The positive stress lobes were observed in the western and northeastern parts of the study area, mainly associated with the Balıkgölü Fault Zone and the Doğubeyazıt Fault. It was important to emphasize that no faults exist west of the study region on the active fault map of Türkiye. These positive stress values may correspond to the epicentral and hypocentral points of microearthquakes. Beneath Tendürek Volcano, the positive stress values appear at shallow depths (2-3 km). The positive and negative stress values, both upward and downward, can be observed with increasing depth, which may correspond to volcanic structure and fault mechanisms. On the other hand, moderate or negative Coulomb stress values were generally observed around the Çaldıran and Erciş faults. When combining existing geological, geochemical, isotopic geochronological, and geomorphological data (Yılmaz et al., 1998; Lebdev et al., 2016a; Ulusoy, 2016; Ünal, 2018), satellite- and InSAR-based deformation observations conducted in and around Tendürek Volcano (Bathke et al., 2013; Gündüz et al., 2023), normal faults related to regional extension, caldera ring faults, regional tectonic regime, and the geological–volcanological characteristics of the region are evaluated alongside the focal mechanism solutions and Coulomb stress change maps obtained in this study, it can be concluded that Tendürek Volcano is potentially active. These findings suggest that future seismic activity could trigger potential magmatic activity. The results presented here are limited to micro-scale seismic data, and multidisciplinary, long-term observations are necessary for wider-scale assessments of volcanic activity. Therefore, Tendürek Volcano and other nearby volcanoes should be monitored

using modern technological methods to track both tectonic and volcanic activity. As a result, more frequent geophysical, geological, and geodetic observations related to Tendürek Volcano are required.

Authors' Contributions
Ayşegül Alkan: Draft Writing, Data Analysis, Investigation, Review & editing. **İsmail Akkaya:** Supervision, Methodology, Review & editing. **Hamdi Alkan:** Conceptualization, Methodology, Original Draft Preparation/Writing

Declaration of Competing Interests
The authors declare no competing interests.

Statement on Research and Publication Ethics
The authors of this article declare that they adhered to research and publication ethics in their work.

Ethics Committee Statement
The authors declare that the materials and methods used in this study did not require ethics committee approval and/or specific legal permission.

Use of Artificial Intelligence
The authors declare that they have not used any type of generative artificial intelligence in the writing of this article, or in the creation of the visuals, figures, tables, or corresponding captions.

References

AFAD. (2025). Disaster and Emergency Management Authority. Erişim tarihi: 25.08.2025. https://deprem.afad.gov.tr/event-catalog

Akın, U., Ulugergerli, E. U., & Kutlu, S. (2014). The assessment of geothermal potential of Turkey by means of heat flow estimation. *Bulletin of the Mineral Research and Exploration*, 149(149), 201-210. https://doi.org/10.19111/bmre.58938

Alkan, H. (2022). Crustal structure in and around the East Anatolian volcanic belt by using receiver functions stacking. *Journal of African Earth Sciences*, 191, 104532. https://doi.org/10.1016/j.jafrearsci.2022.104532

Alkan, H., & Bayrak, E. (2022). Coulomb stress changes and magnitude-frequency distribution for Lake Van region. *Bulletin of the Mineral Research and Exploration*, 168(168), 141-156. https://doi.org/10.19111/bulletinofmre.990666

Alkan, H., Öztürk, S., & Akkaya, İ. (2023). Seismic Hazard Implications in and Around the Yedisu Seismic Gap (Eastern Türkiye) Based on Coulomb Stress Changes, b-Values, and S-wave Velocity, *Pure and Applied Geophysics*, 180 (9), 3227-3248.

Alkan, H., Büyüksaraç, A., & Bektaş, Ö. (2024). Investigation of earthquake sequence and stress transfer in the Eastern Anatolia Fault Zone by Coulomb stress analysis. *Turkish Journal of Earth Sciences*, *33*(1), 56-68. https://doi.org/10.55730/1300-0985.1898

Alkan, A. (2026). Investigation of Coulomb Stress Changes of Microearthquakes in the vicinity of Tendürek Volcano using Focal Mechanism Solutions. (MSc), Yuzuncu Yıl University, Institute of Natural and Applied Science, Van, Turkey.

Asayesh, B. M., Zafarani, H., & Tatar, M. (2020). Coulomb stress changes and secondary stress triggering during the 2003 (Mw 6.6) Bam (Iran) earthquake. *Tectonophysics*, 775, 228304. https://doi.org/10.1016/j.tecto.2019.228304

Bathke, H., Sudhaus, H., Holohan, E. P., Walter, T. R., & Shirzaei, M. (2013). An active ring fault detected at Tendürek volcano by using InSAR. *Journal of Geophysical Research: Solid Earth*, 118(8), 4488-4502. https://doi.org/10.1002/jgrb.50305

Bathke, H., Nikkhoo, M., Holohan, E. P., & Walter, T. R. (2015). Insights into the 3D architecture of an active caldera ring-fault at Tendürek volcano through modeling of geodetic data. *Earth and Planetary Science Letters*, 422, 157-168. https://doi.org/10.1016/j.epsl.2015.03.041

Bektaş, Ö., Ravat, D., Büyüksaraç, A., Bilim, F., & Ateş, A. (2007). Regional geothermal characterisation of East Anatolia from aeromagnetic, heat flow and gravity data. *Pure and Applied Geophysics*, 164(5), 975-998. https://doi.org/10.1007/s00024-007-0196-5

Bektaş, Ö., Alkan, H., Pırtı, A., Yücel, M., & Büyüksaraç, A. (2025). Stress accumulation on the Karlıova (Bingöl) Triple Junction after two big earthquakes (Pazarcık-Ekinözü) in Turkey in 2023. *Bulletin of Geophysics and Oceanography*, 66(2). https://doi.org/10.4430/bgo00485

Büyüksaraç, A., Bektaş, Ö., & Alkan, H. (2024). Fault modeling around southern Anatolia using the aftershock sequence of the Kahramanmaraş earthquakes (Mw= 7.7 and Mw= 7.6) and an interpretation of potential field data. *Acta Geophysica*, *72*(5), 2985-2996. https://doi.org/10.1007/s11600-023-01192-4

Cailleau, B., LaFemina, P. C., & Dixon, T. H. (2007). Stress accumulation between volcanoes: an explanation for intra-arc earthquakes in Nicaragua?. *Geophysical Journal International*, *169*(3), 1132-1138. https://doi.org/10.1111/j.1365-246X.2007.03353.x

Chen, F., Diao, F., Xu, Y., & Xiong, X. (2024) Low-viscosity zones beneath the Coso Volcanic Field revealed by postseismic deformations following the 2019 Ridgecrest earthquake. *Geophysical Research Letters*, 51, e2024GL109566. https://doi.org/10.1029/2024GL109566

Dhar, S., Takada, Y., & Muto, J. (2025). Inferring 3-D rheology of low-viscosity zone around quaternary volcanoes of NE Japan from postseismic deformation of the 2011 Tohoku-Oki earthquake. *Journal of Geophysical Research: Solid Earth*, 130, e2024JB029939. https://doi.org/10.1029/2024JB029939

Emre, Ö., Duman, T. Y., Özalp, S., Şaroğlu, F., Olgun, Ş., Elmacı, H., & Çan, T. (2018). Active fault database of Turkey. *Bulletin of Earthquake Engineering*, 16(8), 3229-3275. https://doi.org/10.1007/s10518-016-0041-2

Ercan, T., Fujitami, T., Madsuda, J. L., Notsu, K., & Ui, T. (1990). Doğu ve Güneydoğu Anadolu Neojen-Kuvaterner volkanitlerine ilişkin yeni jeokjmyasal, radyometrik ve izotopik verilerin yorumu. *Maden Tetkik ve Arama Dergisi*, *110*(110).

Feuillet, N., Cocco, M., Musumeci, C., & Nostro, C. (2006). Stress interaction between seismic and volcanic activity at Mt Etna. *Geophysical Journal International*, *164*(3), 697-718. https://doi.org/10.1111/j.1365-246X.2005.02824.x

Foulger, G. R., Julian, B. R., Hill, D. P., Pitt, A. M., Marlin, P. E., & Shalev, E., (2004), Non-double-couple microearthquakes at Long Valley caldera, California, provide evidence for hydraulic fracturing, *Journal of Volcanol. Geoth. Res.*, 132(45-71).

Gargani, J., Geoffroy, L., Gac, S., & Cravoisier, S. (2006). Fault slip and Coulomb stress variations around a pressured magma reservoir: consequences on seismicity and magma intrusion. *Terra Nova*, 18(6), 403-411. https://doi.org/10.1111/j.1365-3121.2006.00705.x

Gudmundsson, A., Marti, J., & Turon, E. (1997). Stress fields generating ring faults in volcanoes. *Geophysical research letters*, 24(13), 1559-1562. https://doi.org/10.1029/97GL01494

Gülyüz, E., Durak, H., Özkaptan, M., & Krijgsman, W. (2020). Paleomagnetic constraints on the early Miocene closure of the southern Neo-Tethys (Van region; East Anatolia): Inferences for the timing of Eurasia-Arabia collision. *Global and Planetary Change*, 185, 103089. https://doi.org/10.1016/j.gloplacha.2019.103089

Gündüz, H. İ., Yılmaztürk, F., & Orhan, O. (2023). An investigation of volcanic ground deformation using InSAR observations at Tendürek Volcano (Turkey). *Applied Sciences*, *13*(11), 6787. https://doi.org/10.3390/app13116787

Gündüz, H. İ. (2024). *Türkiye'deki aktif volkanlarda meydana gelen yüzey deformasyonlarının jeodezik tekniklerle izlenmesi*. (PhD), Aksaray University, Institute of Natural and Applied Science, Aksaray.

Hardebeck, J. L., & Shearer, P. M. (2002). A new method for determining first-motion focal mechanisms. *Bulletin of the Seismological Society of America*, 92(6), 2264-2276. https://doi.org/10.1785/0120010200

Helffrich, G., Wookey, J., & Bastow, I. (2013). The Seismic Analysis Code. *A Primer and User's Guide* (Cambridge, United Kingdom).

Karakhanian, A., Djrbashian, R., Trifonov, V., Philip, H., Arakelian, S., & Avagian, A. (2002). Holocene-historical volcanism and active faults as natural risk factors for Armenia and adjacent

countries. *Journal of Volcanology and Geothermal Research*, 113(1-2), 319-344. https://doi.org/10.1016/S0377-0273(01)00264-5

Kearney, R. J., Goff, J., Smith, V., Schwab, M. J., Özdemir, Y., Karaoğlu, Ö., ... & Brauer, A. (2025). Glass geochemistry and tephrostratigraphy of key tephra layers in and around Lake Van, Eastern Anatolian Volcanic Province (EAVP). Quaternary Science Reviews, 352, 109165. https://doi.org/10.1016/j.quascirev.2024.109165

Keskin, M. (2003). Magma generation by slab steepening and breakoff beneath a subduction-accretion complex: An alternative model for collision-related volcanism in Eastern Anatolia, Turkey. *Geophysical research letters*, 30(24). https://doi.org/10.1029/2003GL018019

Kiyak, A., Pamuk, E., Köksal, S., Bakar, M. L., & Tosuner, S. (2023). New high resolution aeromagnetic anomaly map of Türkiye and its various derivative-based maps. *Turkish Journal of Earth Sciences*, 32(2), 231-247. https://doi.org/10.55730/1300-0985.1840

Kilb, D., & Hardebeck, J. L. (2006). Fault parameter constraints using relocated earthquakes: a validation of first-motion focal-mechanism data. *Bulletin of the Seismological Society of America*, 96(3), 1140-1158. https://doi.org/10.1785/0120040239

King, G. C., Stein, R. S., & Lin, J. (1994). Static stress changes and the triggering of earthquakes. *Bulletin of the Seismological Society of America*, 84(3), 935-953. https://doi.org/10.1785/BSSA0840030935

Koçyiğit, A., Yilmaz, A., Adamia, S., & Kuloshvili, S. (2001). Neotectonics of East Anatolian Plateau (Turkey) and Lesser Caucasus: implication for transition from thrusting to strike-slip faulting. *Geodinamica Acta*, 14(1-3), 177-195. https://doi.org/10.1080/09853111.2001.11432443

Lebedev, V. A., Sharkov, E. V., Ünal, E., & Keskin, M. (2016a). Late Pleistocene Tendürek volcano (Eastern Anatolia, Turkey): I. Geochronology and petrographic characteristics of igneous rocks. *Petrology*, *24*(2), 127-152. https://doi.org/10.1134/S0869591116020041

Lebedev, V. A., Chugaev, A. V., Ünal, E., Sharkov, E. V., & Keskin, M. (2016b). Late pleistocene tendürek volcano (eastern Anatolia, Turkey). II. Geochemistry and petrogenesis of the rocks. *Petrology*, *24*(3), 234-270. https://doi.org/10.1134/S0869591116030048

Lin, L. C. J., Chuang, R. Y., & Nishimura, T. (2025). Exploring Coulomb stress changes on active structures in Taiwan inferred from decadal GNSS observations. *Earth, Planets and Space*, *77*(1), 88. https://doi.org/10.1186/s40623-025-02215-8

Massa, B., D'Auria, L., Cristiano, E., & De Matteo, A. (2016). Determining the stress field in active volcanoes using focal mechanisms. *Frontiers in Earth Science*, 4, 103. https://doi.org/10.3389/feart.2016.00103

Miller, C. A., Le Mével, H., Currenti, G., Williams-Jones, G., & Tikoff, B. (2017). Microgravity changes at the Laguna del Maule volcanic field: Magma-induced stress changes facilitate mass addition. *Journal of Geophysical Research: Solid Earth*, *122*(4), 3179-3196. https://doi.org/10.1002/2017JB014048

Ottemöller, L., Voss, P.H. and Havskov J. (2021). SEISAN Earthquake Analysis Software for Windows, Solaris, Linux and Macosx, Version 12.0. 607 pp. University of Bergen. ISBN 978-82-8088-501-2, URL http://seisan.info.

Özdemir, Y., Karaoğlu, Ö., Tolluoğlu, A. Ü., & Güleç, N. (2006). Volcanostratigraphy and petrogenesis of the Nemrut stratovolcano (East Anatolian High Plateau): the most recent post-collisional volcanism in Turkey. *Chemical geology*, 226(3-4), 189-211. https://doi.org/10.1016/j.chemgeo.2005.09.020

Özdemir, Y., Mercan, Ç., Oyan, V., & Özdemir, A. A. (2019). Composition, pressure, and temperature of the mantle source region of quaternary nepheline-basanitic lavas in Bitlis Massif, Eastern Anatolia, Turkey: A consequence of melts from Arabian lithospheric mantle. *Lithos*, 328, 115-129. https://doi.org/10.1016/j.lithos.2019.01.020

Öztürk, S. (2017). Space-time assessing of the earthquake potential in recent years in the Eastern Anatolia region of Turkey. *Earth Sciences Research Journal*, 21(2), 67-75. https://doi.org/10.15446/esrj.v21n2.50889

Öztürk, S. (2018). Earthquake hazard potential in the Eastern Anatolian Region of Turkey: seismotectonic b and Dc-values and precursory quiescence Z-value. *Frontiers of Earth Science*, 12(1), 215-236. https://doi.org/10.1007/s11707-017-0642-3

Öztürk, S., & Alkan, H. (2023). Multiple parameter analysis for assessing and forecasting earthquake hazards in the Lake Van region, Turkey. *Baltica*, 36. https://hdl.handle.net/20.500.12440/6116

Pearce, J. A., Bender, J. F., De Long, S. E., Kidd, W. S. F., Low, P. J., Güner, Y., Şaroğlu, F., Yılmaz, Y., Moorbath, S., Mitchell, J. J. (1990). Genesis of collision volcanism in eastern Anatolia Turkey. *J. Volcanol. Geotherm. Res*., 44: 189-229. https://doi.org/10.1016/0377-0273(90)90018-B

Reasenberg, P., & Oppenheimer, D. (1986). *FPFIT, FPPLOT and FPPAGE: Fortran computer programs for calculating and displaying earthquake fault-plane solutions* (Vol. 85, No. 739). US Geological Survey. https://doi.org/10.3133/ofr85739

Reilinger, R., McClusky, S., Vernant, P., Lawrence, S., Ergintav, S., Cakmak, R., et al. (2006). GPS constraints on continental deformation in the Africa-Arabia-Eurasia continental collision zone and implications for the dynamics of plate interactions. *Journal of Geophysical Research*, 111(B5), B05411. https://doi.org/10.1029/2005JB004051

Snoke, J.A. (2003). 85.12 FOCMEC: FOCal MEChanism determinations. *International Geophysics Series*, *81*, 1629-1630.

Suetsugu, D. (1998). Practice on source mechanism, iisee lecture note, *Technical report*, Tsukuba, Japan.

Şen, P. A., Temel, A., & Gourgaud, A. (2004). Petrogenetic modelling of Quaternary post-collisional volcanism: a case study of central and eastern Anatolia. *Geological Magazine*, *141*(1), 81-98. https://doi.org/10.1017/S0016756803008550

Şengör, A. C., & Yilmaz, Y. (1981). Tethyan evolution of Turkey: a plate tectonic approach. *Tectonophysics*, 75(3-4), 181-241. https://doi.org/10.1016/0040-1951(81)90275-4

Şengör, A. M. C., Özeren, S., Genç, T., & Zor, E. (2003). East Anatolian high plateau as a mantle-supported, north-south shortened domal structure. *Geophysical Research Letters*, *30*(24). https://doi.org/10.1029/2003GL017858

Şengör, A. M. C., Tüysüz, O., İmren, C., Sakınç, M., Eyidoğan, H., Görür, N., Pichon, X. L., Rangin, C., Parsons, B., & Tok, B. (2005). The North Anatolian Fault: A new look. *Annual Review of Earth and Planetary Sciences,* *33*(1), 37–112. https://doi.org/10.1146/annurev.earth.32.101802.120415

Şengör, A. C., Özeren, M. S., Keskin, M., Sakınç, M., Özbakır, A. D., & Kayan, İ. (2008). Eastern Turkish high plateau as a small Turkic-type orogen: Implications for post-collisional crust-forming processes in Turkic-type orogens. *Earth-Science Reviews*, 90(1-2), 1-48. https://doi.org/10.1016/j.earscirev.2008.05.002

Tahir, M., Ahmad, Z., Sabahat, S., Mushtaq, M. N., Iqbal, T., Shah, M. A., & Aftab, A. (2024). Source parameters and aftershock pattern of the October 7, 2021, M5.9 Harnai earthquake, Pakistan. *Earthquake Science*, 37(4), 304-323. https://doi.org/10.1016/j.eqs.2024.04.007

Tilling, R. I., & Dvorak, J.J., (1993) Anatomy of a basaltic volcano, *Nature*, 363(125-132).

Toda, S., Stein, R., & Sagiya, T., (2002). Evidence from the AD 2000 Izu islands earthquake swarm that stressing rate governs seismicity, *Nature*, 419(58-61).

Toda, S., Stein, R. S., Sevilgen, V., & Lin, J. (2011). Coulomb 3.3 Graphic-rich deformation and stress-change software for earthquake, tectonic, and volcano research and teaching—user guide. *US Geological Survey open-file report*, 1060(2011), 63. https://pubs.usgs.gov/of/2011/1060

Troise, C., Pingue, F., & De Natale, G. (2003) Coulomb stress changes at calderas: Modeling the seismicity of Campi Flegrei (southern Italy), *Journal of Geophysical Research: Solid Earth*, 108, B6. https://doi.org/10.1029/2002JB002006

Ulusoy, İ. (2016). Temporal radiative heat flux estimation and alteration mapping of Tendürek volcano (eastern Turkey) using ASTER imagery. *Journal of Volcanology and Geothermal Research*, 327, 40-54. https://doi.org/10.1016/j.jvolgeores.2016.06.027

Ünal, E. (2018). Volcanostratigraphy, Petrology and Magmatic Evolution of the Tendürek Volcano, Eastern Turkey. (PhD), Yuzuncu Yıl University, Institute of Natural and Applied Science, Van, Turkey.

Wang, J., Xu, C., Freymueller, J. T., Li, Z., & Shen, W. (2014). Sensitivity of Coulomb stress change to the parameters of the Coulomb failure model: A case study using the 2008 Mw 7.9 Wenchuan earthquake. *Journal of Geophysical Research: Solid Earth*, *119*(4), 3371-3392. https://doi.org/10.1002/2012JB009860

Wessel, P., Luis, J.F., Uieda, L., Scharroo, R., Wobbe, F., Smith, W.H.F., & Tian, D. (2019). The Generic Mapping Tools version 6. *Geochemistry, Geophysics, Geosystems*, *20*, 5556-5564. https://doi:org/10.1029/2019GC008515

Yılmaz, Y., Güner, Y., & Şaroğlu, F. (1998) Geology of The Quaternary Volcanic Centres of The East Anatolia. *Journal of Volcanology and Geothermal Research*, 137 (85): 173-210. https://doi.org/10.1016/S0377-0273(98)00055-9

Yue, C., Qu, C. Y., Li, X. F., Meng, L. Y., Jiang, X. H., & Wu, D. L. (2025). Co-and postseismic stress transfer on different types of faults in Southern Tibet by the 2015 Mw7. 8 Gorkha earthquake. *Journal of Structural Geology*, 191, 105336. https://doi.org/10.1016/j.jsg.2024.105336

Zhou, P., Bastow, I. D., Kounoudis, R., Ogden, C. S., & Wang, Y. (2025). Lithospheric seismic structure of the Anatolian plate and its implications for plateau uplift: Evidence from joint inversion of receiver functions and surface waves. *Geochemistry, Geophysics, Geosystems*, 26, e2025GC012393. https://doi.org/10.1029/2025GC012393